Journal of
Synchrotron
Radiation

ISSN 1600-5775

Received 28 September 2013
Accepted 25 April 2014

Colouration mechanism of underglaze copper-red decoration porcelain (AD 13th–14th century), China

Jian Zhu,[a,b] Huiping Duan,[c] Yimin Yang,[a,b]* Li Guan,[d] Wei Xu,[e] Dongliang Chen,[e] Jing Zhang,[e] Lihua Wang,[f] Yuying Huang[f] and Changsui Wang[a,b]

[a]Key Laboratory of Vertebrate Evolution and Human Origins of Chinese Academy of Sciences, Institute of Vertebrate Paleontology and Paleoanthropology, Chinese Academy of Sciences, Beijing 100044, People's Republic of China, [b]Department of Scientific History and Archaeometry, University of Chinese Academy of Sciences, Beijing 100049, People's Republic of China, [c]School of Materials Science and Engineering, Beijing University of Aeronautics and Astronautics, Beijing 100083, People's Republic of China, [d]Jiangxi Provincial Institute of Cultural Relics and Archaeology, Nanchang 330025, People's Republic of China, [e]Beijing Synchrotron Radiation Facility, Institute of High Energy Physics, Chinese Academy of Sciences, Beijing 100049, People's Republic of China, and [f]Shanghai Synchrotron Radiation Facility, Shanghai Institute of Applied Physics, Chinese Academy of Sciences, Shanghai 201204, People's Republic of China.
*E-mail: yiminyang@ucas.ac.cn

Underglaze copper-red decoration, *i.e.* the copper colourant used to paint diversified patterns on the surface of a body and then covered by transparent glaze and fired at high temperature in a reductive firing environment, is famous all over the world. However, the red colouration mechanism generated by underglaze copper remains unclear. In particular, the fact that the edges of the red patterns are orange has been ignored in previous research. Here, non-destructive analysis has been carried out on a precious fragment of early underglaze red porcelain using synchrotron radiation X-ray fluorescence, X-ray absorption near-edge spectroscopy (XANES) and reflection spectrometry techniques. The results suggest that the copper content in the red region is higher than that in the orange region, and other colour generation elements do not have obvious content difference, indicating that the colour generation effect of the underglaze red product is related to the copper content. XANES analysis shows that the valence states of copper in the red and orange regions are similar and metal copper contributes to their hues. The results of reflection spectrometry demonstrate that tiny orange hues could be attributed to the Mie scatting effect. Therefore, light-scattering effects should be considered when researching the colouration mechanism of underglaze red.

Keywords: XANES; underglaze copper-red decoration; colouration mechanism; reflection spectrometry.

1. Introduction

Although copper was used to provide bright red colours in silicate melts in the Middle East and probably in Mesopotamia at least 3000 years ago, the copper-red effects in Chinese porcelain seem to be an independent ceramic development in terms of production technology, including different chemical compositions and firing temperatures; the most important evidence for this is that the glaze from China is from an earlier period than that from the Middle East (Wood, 1999). Ancient Chinese ceramic products with copper-red are mainly of two types: (i) red glaze, which incorporates copper powder into glaze slurry and is then fired to produce the red colour, such as Jun ware; and (ii) underglaze colour, namely where copper pigments are drawn on the porcelain body and then covered by a layer of transparent glaze and finally fired in a reducing flame at a temperature of around 1473 K. The underglaze colour porcelain has red patterns beneath the glaze and thus is known as 'underglaze copper-red porcelain' or 'underglaze red porcelain'. Genuine underglaze red porcelain emerged in the late Yuan Dynasty (AD 1271–1368), and reached its maturity during the Ming Dynasty (AD 1368–1644); during a lapse of several generations, knowledge of the highly complex porcelain-making processes was lost in the middle of the Ming Dynasty and became more developed and reached its maturity during the Qing Dynasty (AD 1644–1912).

In comparison with other copper-red glaze, the production of underglaze copper-red porcelain was a high-level technique which challenged ancient craftsmen. The firing technique for underglaze copper-red is very rigorous; for example it requires a strong sensitive reduction atmosphere, limited range of firing temperature, proper cooling rate, fine raw materials *etc.*, which made the production of underglaze red porcelain more difficult in the Yuan Dynasty. Therefore, only a limited amount of underglaze red porcelain was successfully produced in early times and all was made in official kilns to satisfy royal demands as imperial wares.

Besides rare intact porcelain, only a few shards of underglaze copper-red porcelain have been excavated, so it is difficult to collect samples for destructive scientific investigation. Until now, there has been little archaeometric research on underglaze red porcelain, and most has focused on the chemical compositions. For example, Tichane (1985) studied the type of pigments on Chinese underglaze red shards from the 14th century and considered that there is sulfide in the pigment in terms of chemical compositions and simulation experiments; thus, he presumed metal copper as the major reason for colour generation. Zhang & Zhang (1997) observed and measured chemical compositions of several sample shards, and found two different painting methods. Obviously, owing to method and sample limitation, the colouring mechanism of underglaze copper-red is not very clear and more scientific analysis is needed. More importantly, the edges of the red patterns often present orange hues in underglaze red porcelain from the Yuan Dynasty, which has been ignored in previous research.

In recent years many spectacular synchrotron experiments have been performed in the field of ancient and historical materials with a strong increase over the past ten years (Bertrand *et al.*, 2011; Cotte *et al.*, 2005). Most major synchrotron techniques are employed in this field, such as X-ray diffraction, X-ray fluorescence, X-ray absorption spectroscopy and computed tomography. Among the investigations performed by exploiting synchrotron radiation, XANES (X-ray absorption near-edge spectroscopy) has proved to be a powerful and flexible tool for culture heritage research in many recent studies (Bardelli *et al.*, 2011; Padovani *et al.*, 2006; Figueiredo *et al.*, 2012; Pradell *et al.*, 2005). It reflects the density of empty states of the absorbing atom, because the near-edge area is affected by the symmetry, the local coordination geometry and the valence of the absorbing atom (Chaboy *et al.*, 2006). Its advantages, *i.e.* it is non-destructive, element-selective, sensitive to trace constituents and applicable to amorphous components, have been gradually regarded and applied in the field of cultural heritage, art and archaeometry in recent years (Wang & Wang, 2011; Bardelli *et al.*, 2012; Robinet *et al.*, 2011; Monnier *et al.*, 2010). More recently, synchrotron radiation XANES has also been successfully employed to identify the valence state of copper in glass and copper-red glaze (Zhu *et al.*, 2012; Silvestri *et al.*, 2012).

As underglaze red shards are very precious, destructive analysis is not permitted. For deeply understanding the colour mechanism of underglaze copper-red, some non-destructive methods including XANES, synchrotron radiation X-ray fluorescence (SRXRF) and reflection spectrometry have been applied to find the differences in element components and colour representation among the different colour regions in order to explain the colouration mechanisms in the orange and red regions of underglaze copper-red.

2. Sample and method

2.1. Sample

The sample (shown in Fig. 1), provided by the Institute of Archaeology of Jiangxi Province and the Institute of Ceramics Archaeology of Jingdezhen, Jiangxi Province (China), was produced in the official kiln of Jingdezhen in the late Yuan Dynasty. The decoration pattern is mainly red but slightly orange at the edge.

2.2. Experimental details

XANES was carried out at beamline 1W1B of Beijing Synchrotron Radiation Facility (BSRF, China). The electron energy of the storage ring was 2.5 GeV and the electron current dropped from 250 mA to 150 mA during the measurements. The size of the beam cast onto the sample position was 0.9 mm × 0.3 mm and its energy resolution was about 1–3 eV. Owing to the low copper concentration in the red decorations and non-destructive purposes, X-ray absorption spectra were collected in fluorescence mode using a Lytle ion-chamber detector. In this paper the energy of the absorption edge (E_0) is defined as the mid-point of the crest in the normalized absorption curve. A Si(111) double-crystal monochromator was employed to scan over the *K*-edge of copper foil at 8979 eV. The incident photon intensity I_0 was monitored by an ion gas chamber and the fluorescent signal was detected by the Lytle ion-chamber detector. The ultimate X-ray absorption spectra of the sample were determined as I_f/I_0. The *K*-edge XANES spectra of the copper standard sample were collected in transmission mode as a reference. XANES spectra were analyzed using the *ATHENA* program in the *IFEFFIT* package (Ravel & Newville, 2005). In this

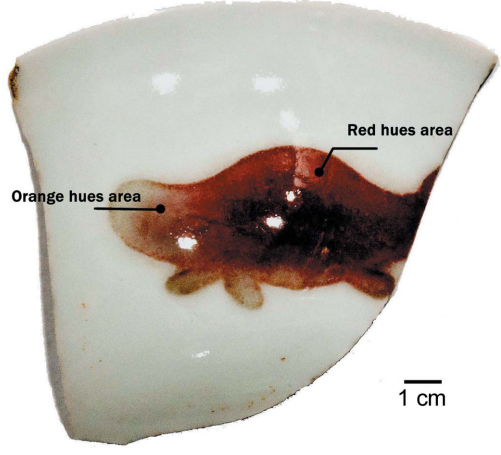

Figure 1
The copper-red underglaze sample and measuring points.

Table 1
Chemical composition of different coloured areas of underglaze copper-red porcelain.

	K (%)	Ca (%)	Ti (%)	Fe (%)	Cr (p.p.m.)	Mn (p.p.m.)	Cu (p.p.m.)	Zn (p.p.m.)	As (p.p.m.)	Rb (p.p.m.)	Pb (p.p.m.)
Red	0.67	2.49	0.02	0.98	18	335	1904	59	685	159	132
Orange	1.11	2.58	0.03	1.44	88	496	869	85	364	216	73
White	0.44	1.37	0.03	0.95	18	279	339	57	0	220	51

study, XANES was employed to identify the valence state of copper in the underglaze red. Furthermore, the measuring points for the XANES were the same as those for the SRXRF, and the XANES spectra were obtained in the fluorescence yield mode. The background absorption of XANES was corrected by subtracting a linear equation that was fitted to the spectral region before the absorption edge.

The SRXRF spectra were recorded at beamline 4W1B at BSRF. The X-ray irradiation area touching the samples was set using adjustable slits, which were fixed at 50 μm × 60 μm. The Si (Li) detector worked under liquid nitrogen and was placed 10 cm from the sample with an energy resolution of about 150–350 eV HWFM. The dead-time rate of the detector was between 20 and 25%. A 2048 multichannel analyzer was used to record and analyze the X-ray fluorescence spectra. Continuous spectrum X-rays in this experiment were adapted for multi-element detection from sodium to uranium with rapid velocity favourable for qualitative analysis of samples. The measuring points on the shard were selected carefully and the chemical composition of the orange and red colour areas was analyzed. A total of 11 elements, including K, Ca, Ti, Cr, Mn, Fe, Cu, Zn, Rb, As and Pb, were measured. Elements with atomic number below 15, such as Si and Al, could not be detected, because their characterized X-rays were absorbed by air in spite of their high content in the porcelain glaze.

Optical spectra were measured using an X-Rite VS450 UV–Vis non-contact benchtop spectrophotometer with a gloss sensor. The measurement conditions included: 45/0° dual illumination, 45° gloss; spectral range 400–700 nm; spectral interval 10 nm. The measuring points were the same for the XANES and SRXRF positions.

3. Results

3.1. SRXRF

The SRXRF results are listed in Table 1. In the red, orange and white regions all the Fe content was lower than 2 wt%. Yang *et al.* (2005) summarized that Fe has no significant influence on the white glaze colour of blue and white porcelain with transparent glaze when the Fe content is lower than 2 wt%. Thus, Fe should not have any influence on the colour of the red and orange hues and the white regions. On the other hand, the Cu content varies in the red and orange hues and the white regions, indicating that the colourization effect is closely related to the copper content and Cu is the main factor of the colour generation effect in underglaze copper-red. Furthermore, the copper content in the red region is higher than that in the orange hues region.

3.2. XANES

The XANES spectra of different regions of the sample and the standard reference copper sample are presented in Fig. 2. Generally, compounds with similar XANES spectra should resemble each other in electron structure. The cuprite (Cu_2O) standard sample has a shoulder peak with a strong intensity at A and a different characteristic peak at D while the main absorption peak of metallic copper divides into two distinct peaks B and C. The positions D and E also express the different characters of the valence. The spectra show that the red and orange regions have very similar patterns, with only a tiny intensity difference.

Shoulder peak (A). It is widely deemed that the shoulder peak for a Cu atom corresponds to the dipole transition $1s \rightarrow 4p$ though it varies between divergent valence states; for example, a shoulder peak at 8975 eV for simple material Cu and at 8980 eV for Cu with 1+ valence. In our experiment the shoulder peak of the orange and red part is near 8980 eV, approximately adjacent to Cu^{1+}. In addition, shoulder peaks for the different coloured areas on the shard display higher intensities than that of the standard sample, indicating that the forbidden transition $1s \rightarrow 4p$ increases due to the decline of coordination symmetry.

Post-edge peak region (B, C). The main edge peak of Cu^0 splits into two crests more clearly than Cu^{1+} at the B (8988 eV) and C (8997 eV) positions, and this is the most obvious distinction of Cu in diverse valence states. The red and orange regions of the sample tend to split into two peaks, but the peaks are displayed weakly. However, these characters at least pronounce metallic copper existing in the coloured areas.

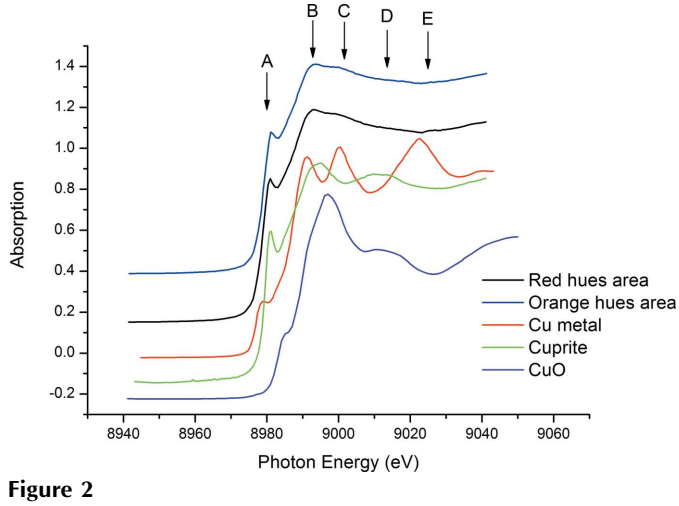

Figure 2
Cu *K*-edge XANES spectra of different areas in the sample.

Post-edge peak (D, E). The XANES spectra at positions D (9010 eV) and E (9019 eV) have shown the comprehensive effect of mixed various valences of copper. The corresponding positions of D and E in the spectrum of the coloured region do not seem to be composed of two distinguishable peaks; this effect is usually caused by different valences coexisting in the sample.

In summary, the spectra of the red and orange regions display a stronger shoulder peak (position A) similar to cuprite (Cu_2O), but the split crest at positions B (8988 eV) and C (8997 eV) shows metallic copper character. In addition, the positions D and E appear to be flatter, and should be influenced by the metallic and monovalent copper state. The CuO spectrum with weak shoulder and main peak position is different for the 0 and 1+ valences of copper and is not found in our results, and divalent copper ions cannot exhibit the red colour in glaze, so there is no obvious 2+ copper existing in the sample. Based on XANES analysis, the various valences of copper exist in the red and orange regions, and the copper existence status in the orange region expresses a similar pattern as that in the red region.

3.3. Reflection spectrum

The reflection spectra of the red and orange regions are shown in Fig. 3, and show that the optical characters of these regions are different. The reflection spectrum of the red region is similar to that of typical red materials, including copper sheet, cinnabar and so on (Wang *et al.*, 2005). However, the reflection spectrum of the orange region is rather flat. Moreover, the main wavelength of the red region is around 650 nm, and that of the orange region is around 620 nm.

4. Discussion and conclusions

The red colour area has a low copper content, suggesting that ancient craftsman probably used a brush for painting. In Chinese tradition, craftsmen drew decorations on porcelain body surfaces, covered the picture with a layer of transparent glaze, and finally put them into a kiln for firing at high temperature.

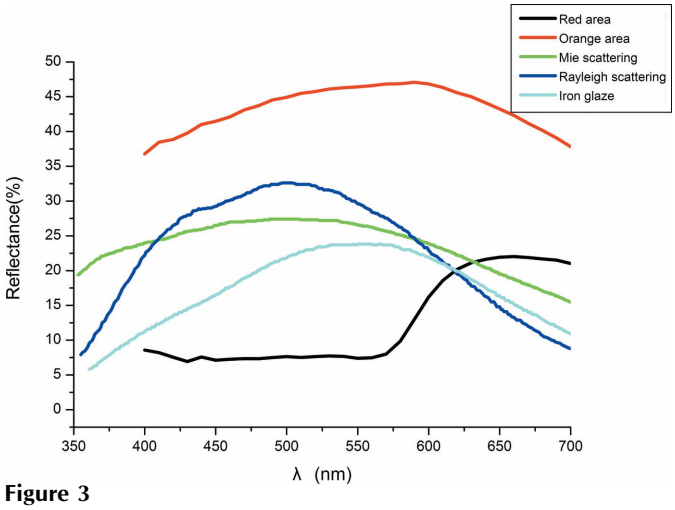

Figure 3
Reflection spectra of the coloured regions of the shard and typical Mie scattering of ancient Chinese porcelain.

Copper nanoparticles contribute to the hues of the red and orange regions, and the red and orange regions have a similar copper status, explaining why their main wavelengths in the reflectance spectra are close. During the firing process for underglaze copper-red the strong reduction atmosphere and high temperature will break the metallic bonds of copper atoms and ionize them. Then the copper ions diffuse into the glassy matrix and are deoxidated to become metallic copper again, growing into copper nanoparticles. Recent research on copper-red recognized that the 2+ valence of copper in glass is reduced to 0/1+ valences in a strong reducing atmosphere, and the copper nanoparticles are commonly considered as the reason for the red colour and also strongly depend on the sizes of the copper particles (Klysubun *et al.*, 2011).

However, the colouration mechanism of the orange hues was still an unsolved question. Why does the edge of the decoration with lower copper content appear as orange hues and not light red? In reflection spectra results the shape of the reflective curve is distinct between the red and orange regions. In particular, the reflectivity of the orange region is higher than that of the red region, and the reflective curve of the orange region varies gently. Given that the nature of copper in the coloured areas is similar, the colour variance should be caused by physical light-scattering effects in the orange region rather than chemical absorption effects.

Light-scatting effects could be caused by minute grains in the glaze, such as undissolved raw material, separation phase droplets, precipitated crystals and air bubbles, which can scatter incident light to deflect from the original direction. There are two kinds of scattering effects in glaze, Rayleigh and Mie scattering, based on the sizes of the scattering particles in the glaze. Rayleigh scattering occurs in particles with sizes much smaller than the wavelength of the incident visible light resulting in a blue colour, while Mie scattering occurs in particles with sizes comparable with or larger than the wavelength of the incident light, resulting in white and opaque colours (Nassau, 1991). In Fig. 3 the reflection curves of typical celadon (Kim *et al.*, 2011), typical blue glaze with Mie scattering and typical blue glaze with Rayleigh scattering (Yang *et al.*, 2005) are presented together to show the influence of Mie scattering and Rayleigh scattering on the reflective curves of iron glaze. Compared with iron glaze (celadon), Mie scattering will make the curve flatter, and Rayleigh scattering will prominently increase the reflectance between 400 and 500 nm in comparison with the intensity of the main wavelength.

In this study, we have considered that the red and orange areas, having similar copper absorption due to the similar nature of copper, and the reflective curve of the orange region is similar to that of typical blue glaze with Mie scattering; furthermore, the reflective curves of iron glaze always show a bell shape. Therefore, it is deduced that the colour of the orange region with lower copper content should be caused by the Mie scattering effect, which plays a more important role in the colouration generation than the absorption effect of

copper and iron in this region. As for what particles contribute to the Mie scattering, only destructive analysis, such as petrographic analysis and SEM observation, will answer this question completely in the future. Moreover, this orange phenomenon is similar to the orange light due to the Mie scattering effect during sunsets and sunrises with red sunglow.

The research presented in this paper has been supported by the National Natural Science Foundation of China (NSFC, Grant No. 11275265). Also, the project was sponsored by the Scientific Research Foundation for the Returned Overseas Chinese Scholars, State Education Ministry, and in part by the President Fund of the UCAS. The research advice on XAFS analysis from Dr Wantana Klysubun (Synchrotron Light Research Institute, Thailand) is especially appreciated.

References

Bardelli, F., Barone, G., Crupi, V., Longo, F., Maisano, G., Majolino, D., Mazzoleni, P. & Venuti, V. (2012). *J. Synchrotron Rad.* **19**, 782–788.

Bardelli, F., Barone, G., Crupi, V., Longo, F., Majolino, D., Mazzoleni, P. & Venuti, V. (2011). *Anal. Bioanal. Chem.* **399**, 3147–3153.

Bertrand, L., Languille, M.-A., Cohen, S. X., Robinet, L., Gervais, C., Leroy, S., Bernard, D., Le Pennec, E., Josse, W., Doucet, J. & Schöder, S. (2011). *J. Synchrotron Rad.* **18**, 765–772.

Chaboy, J., Muñoz-Páez, A. & Sánchez Marcos, E. (2006). *J. Synchrotron Rad.* **13**, 471–476.

Cotte, M., Dumas, P., Richard, G., Breniaux, R. & Walter, Ph. (2005). *Anal. Chim. Acta*, **553**, 105–110.

Figueiredo, M. O., Silva, T. P. & Veiga, J. P. (2012). *J. Electron Spectrosc. Relat. Phenom.* **185**, 97–102.

Kim, J. Y., No, H. G., Jeon, A. Y., Kim, U. S., Pee, J. H., Cho, W. S., Kim, K. J., Kim, C. M. & Kim, C. S. (2011). *Ceram Int.* **37**, 3389–3395.

Klysubun, W., Thongkam, Y., Pongkrapan, S., Won-in, K., Thienprasert, J. T. & Dararutana, P. (2011). *Anal. Bioanal. Chem.* **399**, 3033–3040.

Monnier, J., Reguer, S., Vantelon, D., Dillmann, P., Neff, D. & Guillot, I. (2010). *Appl. Phys. A*, **99**, 399–406.

Nassau, K. (1991). *The Physics and Chemistry of Color.* Beijing: Science Press.

Padovani, S. *et al.* (2006). *Appl. Phys. A*, **83**, 521–528.

Pradell, T., Molera, J., Roque, J., Vendrell-Saz, M., Smith, A. D., Pantos, E. & Crespo, D. (2005). *J. Am. Ceram. Soc.* **88**, 1281–1289.

Ravel, B. & Newville, M. (2005). *J. Synchrotron Rad.* **12**, 537–541.

Robinet, L., Spring, M., Pagès-Camagna, S., Vantelon, D. & Trcera, N. (2011). *Anal. Chem.* **83**, 5145–5152.

Silvestri, A., Tonietto, S., D'Acapito, F. & Molin, G. (2012). *J. Cult. Herit.* **13**, 137–144.

Tichane, R. (1985). *Red, Reds Copper Reds*, pp. 49–55. New York: The New York Institute for Glaze Research.

Wang, L. H. & Wang, C. S. (2011). *J. Anal. At. Spectrom.* **26**, 1796–1801.

Wang, L. Q., Liang, G.-Z., Dang, G.-C. & Wang, F. (2005). *Spectrosc. Spectr. Anal.* **25**, 1293–1296.

Wood, N. (1999). *Chinese Glazes: Their Origins, Chemistry and Recreation*, pp 167–168. University of Pennsylvania Press.

Yang, Y. M., Feng, M., Ling, X., Mao, Z., Wang, C., Sun, X. & Guo, M. (2005). *J. Archaeol. Sci.* **32**, 301–310.

Zhang, F. K. & Zhang, P. S. (1997). *Proceedings of the International Symposium on Ancient Ceramics (IPAC95)*, pp. 197–198. Shanghai, People's Republic of China.

Zhu, J., Yang, Y., Xu, W., Chen, D., Dong, J., Wang, L. & Glascock, M. D. (2012). *X-ray Spectrom.* **41**, 363–366.